



Synthesis of Adaptive Neuro-Fuzzy Control Algorithms for a Class of Autonomous Aerial Vehicles

T. Tuan Don¹, N. Quang Hung², N. Quang Vinh³, P. Quang Hieu³
and N. Tat Tuan^{4*}

¹ Academy of Military Science and Technology, Ha Noi, Vietnam

² East Asia University of Technology (EAUT), Ha Noi, Vietnam

³ Missile-Ship Artillery Department, Naval Academy, Khanh Hoa, Vietnam

⁴ Le Quy Don Technical University, Ha Noi, Vietnam

The manuscript was received on 4 June 2024 and was accepted
after revision for publication as an original research paper on 13 June 2025.

Abstract:

Autonomous flying devices (AFDs) in the Navy are modern flying devices widely used in the military sector as the flying device changes speed and altitude, its kinematic characteristics vary significantly, requiring a controller capable of adapting to these changes. Therefore, this paper presents a method for synthesizing an adaptive fuzzy neural network control algorithm for autonomous naval flying devices to stabilize the desired characteristic angles. A Matlab/Simulink environment survey is conducted with assumed parameters and the results are compared with those of a PID controller to highlight the advantages of the proposed algorithm.

Keywords:

missile, neural network, fuzzy control, adaptive control

1 Introduction

Autonomous flying devices (AFDs) such as missiles and UAVs are widely used in the military and the Navy. The study [1], based on adaptive control theory with a nonlinear flying device dynamic model, designs an autopilot system for a class of missiles during the launch phase to adapt to changes in aerodynamic parameters and wind effects. However, the flying device dynamic model in [1] has been linearized into a transfer function form. Study [2] applies model predictive control to design a missile control system, but the author of [2] also uses a linear stationary missile model to build the control algorithm. Study [3] uses classical control theory (PID control) to synthesize the control law, but the published results do not specifically address the influence of environmental factors or changes in the kinematic properties

* Corresponding author: Aerospace Control Systems, Le Quy Don University, 236 Hoang Quoc Viet, Ha Noi, Vietnam. Phone +849 81 78 36 68, E-mail: nguyentattuan@lqdu.edu.vn. ORCID 0000-0002-7908-4336.

of UAVs. Neural networks and fuzzy systems are currently widely applied in control and have achieved significant results. Numerous adaptive control methods for nonlinear systems are based on either fuzzy systems [4-5] or neural networks [6-7]. In [8], a multilayer neural network-based output feedback controller is implemented, utilizing state observer gain to estimate the time derivative of the system output. In [9-10], a close combination of fuzzy systems and neural networks is used to approximate functions with output feedback control laws. Building on these foundations, an adaptive fuzzy neural network output feedback controller can be developed for uncertain nonlinear systems using only measurable system output. This approach ensures that all signals are bounded and that the system's closed-loop output converges to the desired trajectory.

Building on the theory of adaptive fuzzy neural network output feedback controllers, the authors have developed an adaptive fuzzy neural network control law specifically for a class of naval flying devices to stabilize their desired characteristic angles. Section one presents the mathematical model of the flying device; section two presents the method for synthesizing the adaptive fuzzy neural network control law. Section three presents simulation results with assumed parameters [11].

2 Object Model

Consider a model of a flying device in space as shown in Fig. 1 [11].

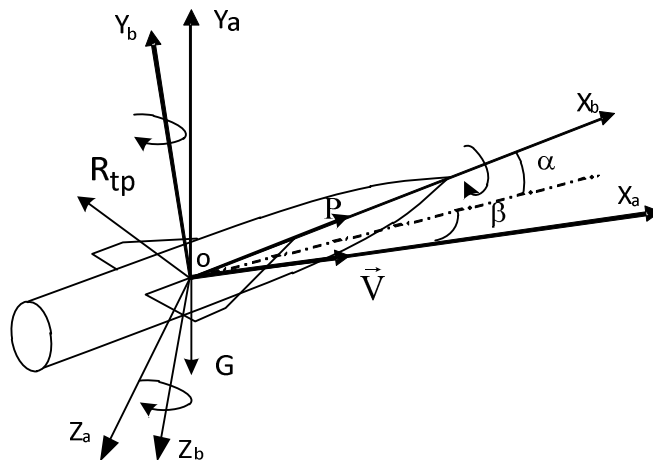


Fig. 1 Description of the rotational motion of the fly device

In which $Ox_b Y_b Z_b$ corresponding to the axes of the coordinate system attached to the object (linked coordinate system); $Ox_a Y_a Z_a$ speed coordinate system; α , β , γ , ψ the angles corresponding to the angle of attack, sideslip angle, roll angle, and heading angle of the flying device.

The orbital coordinate system $Ox_m Y_m Z_m$ is a coordinate system attached to the autonomous flight device (AFD), with the origin located at the center of mass of the AFD (O). The Ox_m axis aligns with the velocity vector \vec{V}_m of the AFD relative to the ground coordinate system, also known as the ground velocity vector. The $(Ox_m Y_m)$ plane is perpendicular to the horizontal plane corresponding to the position of

O relative to the Earth, while the OZ_m axis is perpendicular to the OX_mY_m plane, forming a right-handed orthogonal coordinate system. As such, the orbital coordinate system maintains a relatively stable position concerning the ground in the area where the AFD is flying, depending solely on the motion of the AFD's center of mass.

According to Newton's second law, the translational motion equations of the center of mass of the flying device and the rotational motion around the flying device are determined [11]:

$$m \frac{d\vec{V}_m}{dt} = \sum \vec{F} \tag{1}$$

$$\frac{d\vec{K}}{dt} = \sum \vec{M} \tag{2}$$

where $\sum \vec{F}$ [N] is the total vector of all external forces acting on the flying device of mass m [kg]; $d\vec{V}_m/dt$ is the total acceleration vector of the ground speed vector \vec{V}_m [m/s] in the ground coordinate system; $\sum \vec{M}$ [kg·m²/s²] is the total vector of external moments acting on the flying device; \vec{K} [kg·m²/s] is the angular momentum.

The total acceleration of the flying device in the ground coordinate system is determined [11]:

$$\frac{d\vec{V}_m}{dt} = \frac{\tilde{d}\vec{V}_m}{dt} + \vec{\omega}_m \vec{V}_m \tag{3}$$

where $d\vec{V}_m/dt$ is the total derivative of the vector \vec{V}_m concerning time; $\tilde{d}\vec{V}_m/dt$ is the relative derivative of the vector \vec{V}_m in the rotating reference frame; $\vec{\omega}_m$ (degree/s) is the angular velocity vector of the orbital coordinate system.

Since in the orbital coordinate system $V_{xm} = V_m$, $V_{ym} = 0$, $V_{zm} = 0$, Eq. (1) is developed into Eqs:

$$m \frac{dV_m}{dt} = \sum F_{xm} \tag{4}$$

$$mV_m \frac{d\theta}{dt} = \sum F_{ym} \tag{5}$$

$$-mV_m \frac{d\Psi}{dt} \cos \theta = \sum F_{zm} \tag{6}$$

Developing Eqs (4), (5), and (6) we have:

$$m \frac{dV_m}{dt} = P \cos \alpha \cos \beta - R_{xa} - G \sin \theta \tag{7}$$

$$mV_m \frac{d\theta}{dt} = P(\sin \alpha \cos \gamma_a + \cos \alpha \sin \beta \sin \gamma_a) + R_{ya} \cos \gamma_a - R_{za} \sin \gamma_a - G \cos \theta \tag{8}$$

$$-mV_m \frac{d\Psi}{dt} \cos \theta = P(\sin \alpha \sin \gamma_a - \cos \alpha \sin \beta \cos \gamma_a) + R_{ya} \sin \gamma_a + R_{za} \cos \gamma_a \tag{9}$$

In which θ is the trajectory angle of the flying device, γ_a is the inclination angle of the velocity coordinate system relative to the linked coordinate system, P is the thrust along the engine's axis; R_{xa} , R_{ya} , R_{za} are the aerodynamic drag forces.

Developing Eq. (2) in the linked coordinate system:

$$\frac{d\omega_x}{dt} = J_x^{-1} \left[\sum M_{xb} - (J_z - J_y) \omega_y \omega_z \right] \quad (10)$$

$$\frac{d\omega_y}{dt} = J_y^{-1} \left[\sum M_{yb} - (J_x - J_z) \omega_x \omega_z \right] \quad (11)$$

$$\frac{d\omega_z}{dt} = J_z^{-1} \left[\sum M_{zb} - (J_y - J_x) \omega_x \omega_y \right] \quad (12)$$

where M_{xb} , M_{yb} , M_{zb} [$\text{kg}\cdot\text{m}^2/\text{s}^2$] is the vector of external moments acting on the flying device along the axes of the linked coordinate system; ω_x , ω_y , ω_z , [degree/s] are the angular velocities around the center of mass of the flying device in the linked coordinate system; J_x , J_y , J_z [$\text{kg}\cdot\text{m}^2$] are the moments of inertia along the axes.

The dynamic equations describing the rotational motion of the flying device in the linked coordinate system have the form:

$$\frac{d\psi}{dt} = \frac{1}{\cos \vartheta} (\omega_y \cos \gamma - \omega_z \sin \gamma) \quad (13)$$

$$\frac{d\vartheta}{dt} = \omega_y \sin \gamma + \omega_z \cos \gamma \quad (14)$$

$$\frac{d\gamma}{dt} = \omega_x - \text{tg} \vartheta (\omega_y \cos \gamma - \omega_z \sin \gamma) \quad (15)$$

where the angles ψ , ϑ , γ are the heading, pitch, and roll angles of the flying device.

2.1 Model of Rotational Motion of the Flying Device in the Vertical Channel

When the roll angle is stabilized at the value $\gamma = 0$, $\gamma_a \approx \gamma$, Eq. (8) has the form:

$$mV \frac{d\theta}{dt} = P \sin \alpha + R_{ya} - G \cos \theta \quad (16)$$

$$mV \frac{d\theta}{dt} = P\alpha + \left(C_y^\alpha \alpha + C_y^{\delta_c} \delta_c \right) \frac{\rho V^2 S}{2} - G \cos \theta \quad (17)$$

where $R_{ya} = C_{ya} q S = \left(C_y^\alpha \alpha + C_y^{\delta_c} \delta_c \right) q S$ with $q = 1/2 \rho V^2$ [kg/m^3] as the air density; V is the flight speed relative to undisturbed air; S [m] is the characteristic area of the missile; C_{ya} is the lift coefficient; δ_c [degree] is the angle of the lift control surface.

For a class of missiles being considered, the component $C_y^{\delta_c} \delta_c$ is very small compared to $C_y^\alpha \alpha$, so it can be neglected, and Eq. (17) will have the form:

$$V \frac{d\theta}{dt} = \frac{P + C_y^\alpha \frac{\rho V^2 S}{2}}{m} \alpha - g \cos \theta \quad (18)$$

where g is the gravitational acceleration ($g = 9.8 \text{ m/s}^2$).

The left side of Eq. (18) is the normal acceleration of the moving object; the first term on the right side is the normal acceleration of the flying device created to control the vertical channel. This is the parameter required to accurately track the target. The optimal angle of attack must be determined to control the flying device accurately in the terminal guidance phase.

The relationship between the angles characteristic of the motion of the rocket is presented in the following expression [8]:

$$\sin \theta = \sin \vartheta \cos \alpha \cos \beta - \cos \vartheta \cos \gamma \sin \alpha \cos \beta - \cos \vartheta \sin \gamma \sin \beta \quad (19)$$

In the self-guided approach mode, AFDs typically fly with a small pitch angle α and a small side slip angle β . The heading angle ψ , yaw angle ϑ , trajectory tilt angle θ , and trajectory heading angle Ψ also have small values. When these conditions are satisfied, the following approximations can be made: $\sin \alpha \approx \alpha$, $\sin \beta \approx \beta$, $\sin \theta \approx \theta$, $\sin \psi \approx \psi$, $\sin \Psi \approx \theta$, $\cos \alpha \approx 1$, $\cos \beta \approx 1$, $\cos \psi \approx 1$, $\cos \theta \approx 1$, $\cos \Psi \approx 1$.

When $\gamma \approx 0$, Eq. (19) takes the following form [12]:

$$\theta = \vartheta - \alpha \quad (20)$$

Differentiating both sides of Eq. (20) we get:

$$\dot{\alpha} = \dot{\vartheta} - \dot{\theta} \quad (21)$$

From Eq. (18), rewriting:

$$\dot{\theta} = \frac{P + C_y \frac{\rho V^2 S}{2}}{mV} \alpha - \frac{g \cos \theta}{V} \quad (22)$$

Under the condition that the roll angle (Cren) is stabilized around the value $\gamma = 0$, and considering the pitch angle generated by rotation around the OZ axis:

$$\dot{\vartheta} = \frac{d\vartheta}{dt} = \omega_z \quad (23)$$

Eq. (12) becomes:

$$\dot{\omega}_z = J_z^{-1} M_{zb} \quad (24)$$

Developing Eq. (24) we have:

$$\dot{\omega}_z = \frac{1}{2} J_z^{-1} m_{zb}^{\alpha} \rho V_m^2 S L_c \alpha + \frac{1}{2} J_z^{-1} m_{zb}^{\omega_z} \rho V_m^2 S_{cl} L^2 \omega_z + \frac{1}{2} J_z^{-1} m_{zb}^{\delta_c} \rho V_m^2 S_{cl} L_{cl} \delta_c \quad (25)$$

Substituting Eqs (20) and (22) into Eq. (21):

$$\dot{\alpha} = \omega_z - \frac{P + C_y \frac{\rho V^2 S}{2}}{mV} \alpha + \frac{g}{V} \cos(\vartheta - \alpha) \quad (26)$$

Differentiating both sides of Eq. (26):

$$\ddot{\alpha} = \left(\frac{1}{2} J_z^{-1} m_{zb}^{\alpha} \rho V_m^2 S L_c \alpha + \frac{1}{2} J_z^{-1} m_{zb}^{\omega_z} \rho V_m^2 S_{cl} L^2 \omega_z + \frac{1}{2} J_z^{-1} m_{zb}^{\delta_c} \rho V_m^2 S_{cl} L_{cl} \delta_c \right) - \frac{P + C_y \frac{\rho V^2 S}{2}}{mV} \dot{\alpha} - \frac{g}{V} \sin \theta \left(\frac{P + C_y \frac{\rho V^2 S}{2}}{mV} \alpha - \frac{g}{V} \cos \theta \right) \quad (27)$$

Substituting $\dot{\vartheta} = \omega_z$ into Eq. (27) we get:

$$\ddot{\alpha} = \left(\frac{1}{2} J_z^{-1} m_{zb}^{\alpha} \rho V^2 S L_c \alpha + \frac{1}{2} J_z^{-1} m_{zb}^{\omega_z} \rho V^2 S_{cl} L^2 \dot{\vartheta} + \frac{1}{2} J_z^{-1} m_{zb}^{\delta_c} \rho V^2 S_{cl} L_{cl} \delta_c \right) - \frac{P + C_y^{\alpha} \frac{\rho V^2 S}{2}}{mV} \dot{\alpha} - \frac{g}{V} \sin \theta \left(\frac{P + C_y^{\alpha} \frac{\rho V^2 S}{2}}{mV} \alpha - \frac{g}{V} \cos \theta \right) \tag{28}$$

We set:

$$\left\{ \begin{array}{ll} k_{12} = \frac{P + C_y^{\alpha} \frac{\rho V^2 S}{2}}{mV} & k_{22} = \frac{m_{zb}^{\alpha} \rho V^2 S L_c}{2 J_z} \\ k_{32} = \frac{m_{zb}^{\omega_z} \rho V S_{cl} L^2}{2 J_z} & k_{42} = \frac{m_{zb}^{\delta_c} \rho V^2 S_{cl} L_{cl}}{2 J_z} \end{array} \right.$$

Substituting $\theta = \vartheta - \alpha$ into Eq. (28) we get:

$$\ddot{\alpha} = k_{22} \alpha - \frac{g}{V} k_{12} \alpha \sin(\vartheta - \alpha) - k_{12} \dot{\alpha} + k_{32} \dot{\vartheta} + \left(\frac{g}{V} \right)^2 \sin(\vartheta - \alpha) \cos(\vartheta - \alpha) + k_{42} \delta_c \tag{29}$$

By combining Eqs (25) and (29), we obtain the system of Eqs:

$$\left\{ \begin{array}{l} \ddot{\alpha} = k_{22} \alpha - \frac{g}{V} k_{12} \alpha \sin(\vartheta - \alpha) - k_{12} \dot{\alpha} + k_{32} \dot{\vartheta} + \left(\frac{g}{V} \right)^2 \sin(\vartheta - \alpha) \cos(\vartheta - \alpha) + k_{42} \delta_c \\ \ddot{\vartheta} = k_{22} \alpha + k_{32} \dot{\vartheta} + k_{42} \delta_c \end{array} \right. \tag{30}$$

Define the state variable:

$$\left\{ \begin{array}{l} x_1 = \alpha \\ x_2 = \dot{x}_1 = \dot{\alpha} \\ x_3 = \vartheta \\ x_4 = \dot{x}_3 = \dot{\vartheta} \end{array} \right.$$

We see that $u = \delta_c$ is the control input; the output is $x_1 = \alpha$, Eq. (30) is rewritten in the form:

$$\left\{ \begin{array}{l} \dot{x} = A_0 x + B_0 [F(x) + G(x)u + d] \\ y = C_0^T x \end{array} \right. \tag{31}$$

where $A_0 = \text{diag}[A_1, A_2]$; $B_0 = \text{diag}[B_1, B_2]$; $C_0 = \text{diag}[C_1, C_2]$

$$A_k = \begin{bmatrix} 0 & 1 \\ 0 & 0 \end{bmatrix}; B_k = \begin{bmatrix} 0 \\ 1 \end{bmatrix}; C_k = \begin{bmatrix} 0 \\ 1 \end{bmatrix}$$

$$\begin{cases} F(x) = [f_1(x), f_2(x)]^T \\ G(x) = [g_1(x), g_2(x)]^T \end{cases}$$

$$f_1(x) = k_{22}\alpha - \frac{g}{V}k_{12}\alpha \sin(\vartheta - \alpha) - k_{12}\dot{\alpha} + k_{32}\dot{\vartheta} + \left(\frac{g}{V}\right)^2 \sin(\vartheta - \alpha) \cos(\vartheta - \alpha)$$

$$f_2(x) = k_{22}\alpha + k_{32}\dot{\vartheta}$$

$$g_1(x) = g_2(x) = k_{42}$$

d is the external disturbance affecting the system.

3 LQ Controller

The LQ controller is an optimal solution for linear systems. By combining Eqs (25) and (26), we obtain the following system of Eqs:

$$\begin{cases} \dot{\alpha} = \omega_z - \left(\frac{P + C_y^\alpha \frac{\rho V^2 S}{2}}{Vm} \right) \alpha + \frac{g \cos \theta}{V} \\ \dot{\omega}_z = m_{zb}^\alpha \frac{\rho V^2 S L_c}{2J_z} \alpha + m_{zb}^{\omega_z} \frac{\rho V S_{cl} L_c^2}{2J_z} \omega_z + m_{zb}^{\delta_c} \frac{\rho V^2 S_{cl} L_c}{2J_z} \delta_c \end{cases} \quad (32)$$

To solve the problem using the LQ method, the system (32) is linearized around the equilibrium state.

We set: $x = [x_1 \ x_2]^T = [\alpha \ \omega_z]^T$; $u_c = \delta_c$

The linear state equation is in the form:

$$\begin{cases} \dot{x} = A_{lq}x + B_{lq}u \\ y = Dx \end{cases} \quad (33)$$

where A_{lq} and B_{lq} are determined by the following expressions:

$$A_{lq} = \left. \frac{\partial f}{\partial x} \right|_{x=0, u=0} = \begin{bmatrix} -k_{12} & 1 \\ k_{22} & k_{32} \end{bmatrix}; B_{lq} = \left. \frac{\partial f}{\partial x} \right|_{x=0, u=0} = \begin{bmatrix} 0 \\ k_{42} \end{bmatrix}; D = [1 \ 0]$$

Let the error between the output response y and the desired signal y_c be a new state variable, we have:

$$\dot{e}_y = y_c - y = y_c - Dx \quad (34)$$

The extended state-space model with the addition of the state variable e_y is:

$$\begin{bmatrix} \dot{x} \\ \dot{e}_y \end{bmatrix} = \begin{bmatrix} A_{lq} & 0_{2 \times 1} \\ -D & 0 \end{bmatrix} \begin{bmatrix} x \\ e_y \end{bmatrix} + \begin{bmatrix} B \\ 0 \end{bmatrix} + \begin{bmatrix} 0_{2 \times 1} \\ 1 \end{bmatrix} y_c \quad (35)$$

where $X = [x \ e_y]^T$; $A_{lqe} = \begin{bmatrix} A_{lq} & 0_{2 \times 1} \\ -D & 0 \end{bmatrix}$

$$B_{lqe} = \begin{bmatrix} B_{lq} \\ 0 \end{bmatrix}; B_y = \begin{bmatrix} 0_{2 \times 1} \\ 1 \end{bmatrix}; D_e = [D \ 0]$$

We have

$$\begin{cases} \dot{X} = A_{lqe}X + B_{lqe}u + B_y y_c \\ y = D_e X \end{cases} \quad (36)$$

The problem is to find the optimal control law u_{lq}^* for the system (36) to minimize the quadratic quality index function:

$$J = \frac{1}{2} \int_0^{\infty} [X^T Q X + u R u] dt \rightarrow \min \quad (37)$$

where Q and R are the weighting matrices for the state variable and the control variable ($Q \geq 0, R \geq 0$).

Eq. (37) represents the desire to minimize the error e_y (the output of the system following the reference signal) and to minimize the control variable.

The problem is solved by using the Lagrange multiplier $\lambda(t)$ and establishing the Hamiltonian function:

$$H = \frac{1}{2} X^T Q X + \frac{1}{2} u R u + \lambda^T (A_{lqe} X + B_{lqe} u) \quad (38)$$

According to the established conditions, the optimal control variable u^* satisfies:

$$u_{lq}^*(t) = -R^{-1} B_{lqe}^T \lambda(t) \quad (39)$$

where

$$\lambda(t) = P(t) X \quad (40)$$

where $P(t)$ is the solution of the Riccati differential equation:

$$\begin{cases} \dot{P}(t) = -P(t) A_{lqe} - A_{lqe}^T P(t) + P(t) B_{lqe}^T R^{-1} B_{lqe} P(t) - Q \\ P(0) = P_0 \end{cases} \quad (41)$$

Let $K_{op}^T = -R^{-1} B_{lqe}^T P(t)$, the optimal control law (38):

$$u_{lq}^*(t) = K_{op}^T X(t), K_{op} \in R^{3 \times 1} \quad (42)$$

4 Direct Adaptive Controller (NFC)

Consider the state equation of the form [9]:

$$\begin{cases} \dot{x} = A_0 x + B_0 [F(x) + G(x)u + d] \\ y = C_0^T x \end{cases} \quad (43)$$

Eq. (43) has the control law [9, 15]:

$$u^* = \frac{1}{G(x)} [-F(x) + y_r^{(m)} + K_c^T e] \quad (44)$$

where $y_r^{(m)}$ is the reference signal and e is the deviation.

In reality, the mathematical models of controlled objects cannot be exact, so the ideal control law (44) cannot be implemented.

Moreover, the automated aerial vehicle only measures the output y . Therefore, a state observer must be constructed to estimate the state of the system.

$$\begin{cases} \dot{\hat{e}} = A_0 \hat{e} - B_0 K_c^T \hat{e} + K_0 (E_1 - \hat{E}_1) \\ \hat{E}_1 = C_0^T \hat{e} \end{cases} \quad (45)$$

From this, the problem is solved by directly identifying the ideal control law $u^*(t)$ using the fuzzy neural network with input parameters as the estimation errors \hat{e} . This controller can operate according to the following equation:

$$u = u_f + u_{nh} \quad (46)$$

in which

$$\begin{cases} u_f = [u_{f1}, u_{f2}, \dots, u_{fp}]^T \in R^p \\ u_{nh} = [u_1, u_2, \dots, u_p]^T \in R^p \end{cases}$$

where u_f is the ideal control law identified based on the output of the fuzzy neural network; the component u_{nh} serves as noise reduction and error compensation for the object model.

The fuzzy neural network is used to approximate the nonlinear functions. In developing the controller for the object, the author employs a fuzzy neural network with the structure depicted in Fig. 2.

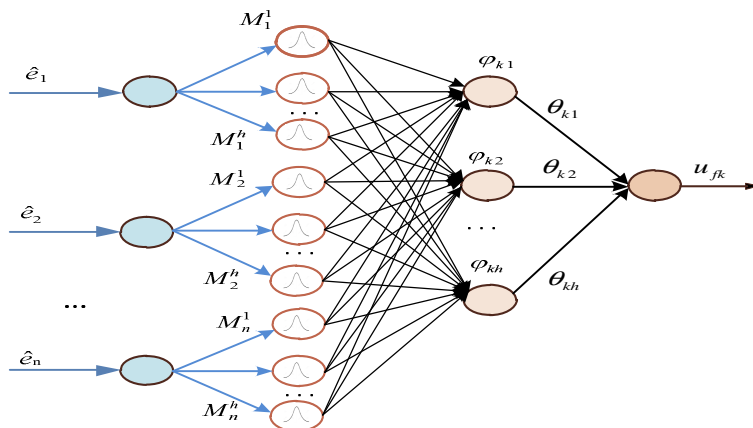


Fig. 2 Structure of the fuzzy neural network approximator

The basic configuration of a neuro-fuzzy approximator consists of several If-Then rules and a fuzzy inference mechanism. The If-Then Law i (with $i = 1 \div h$) is written:

R_i : If \hat{e}_1 is M_{k1}^i and \hat{e}_2 is M_{k2}^i and ... then u_{fk} is B_k^i ; where $M_{k1}^i, M_{k2}^i, \dots, B_k^i$ are fuzzy sets.

The Singleton neural fuzzy function approximator has four layers:

Layer 1 includes inputs, representing the input language vector $\hat{e}_k = [\hat{e}_1, \hat{e}_2, \dots, \hat{e}_n]^T$; layer 2 represents the member function value of the total number of language

variables, each node of layer 2 implements the member function value $\mu_{M_k^i} = \prod_{j=1}^n \mu_{M_{kj}^i}(\hat{e}_{kj})$; layer 3 are the nodes of the fuzzy base vector, the fuzzy base vector $\phi_k(\hat{e}) = [\phi_{k1}, \phi_{k2}, \dots, \phi_{kh}]^T \in R^h$, where ϕ_{ki} is the value of the output of each

node of layer 3 $\phi_{ki}(\hat{e}_k) = \frac{\prod_{j=1}^n \mu_{M_{kj}^i}(\hat{e}_j)}{\sum_{i=1}^h \left[\prod_{j=1}^n \mu_{M_{kj}^i}(\hat{e}_j) \right]}$ (with $i = 1 \div h$); Layer 4 output represents

the output value of the network u_{jk} , layer 3 and layer 4 connection weights $\Omega_k = [\Omega_{k1}, \Omega_{k2}, \dots, \Omega_{kh}]^T \in R^h$, these parameters can be adaptively adjusted. Using the max-prod inference rule, fuzzification, and defuzzification according to the centroid average, the output of the fuzzy-neural approximator can be expressed as follows:

$$u_{jk} = \frac{\sum_{i=1}^h \Omega_{ki} \left[\prod_{j=1}^n \mu_{M_{kj}^i}(\hat{e}_{kj}) \right]}{\sum_{i=1}^h \left[\prod_{j=1}^n \mu_{M_{kj}^i}(\hat{e}_{kj}) \right]} = \Omega_k^T \phi_k(\hat{e}) \tag{47}$$

From that, we can construct the block diagram for the adaptive neuron-fuzzy controller as shown in Fig. 3 below.

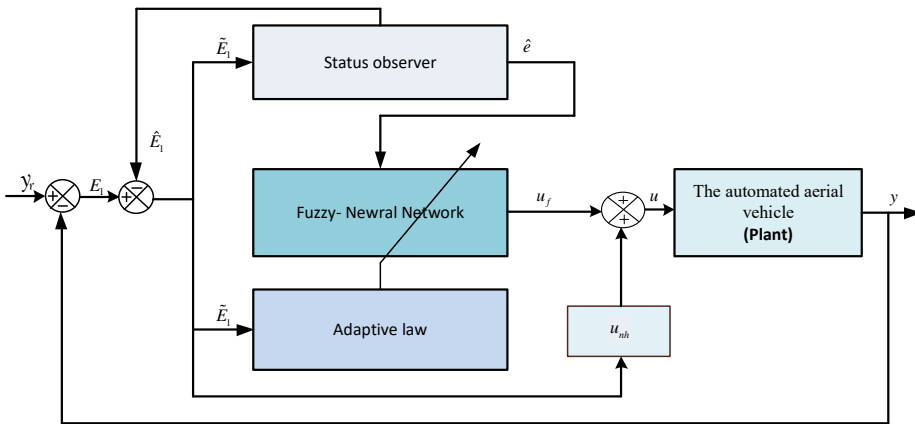


Fig. 3 Block diagram of the adaptive neuron-fuzzy controller

The weights of the network Ω_k are updated according to the adaptive updating rule [13]:

$$\dot{\Omega}_k = \begin{cases} \gamma_k \tilde{E}_{k1} \phi_k(\hat{e}_k) & \text{if } \|\Omega_k\| < m_{\Omega_k} \text{ or } (\|\Omega_k\| = m_{\Omega_k} \text{ and } \tilde{E}_{k1} \Omega_k^T \phi_k(\hat{e}_k) \geq 0) \\ \text{Pr}[\gamma_k \tilde{E}_{k1} \phi_k(\hat{e}_k)] & \text{if } \|\Omega_k\| = m_{\Omega_k} \text{ and } \tilde{E}_{k1} \Omega_k^T \phi_k(\hat{e}_k) < 0 \end{cases} \tag{48}$$

with $\gamma_k > 0$ is a design adaptation parameter.

When $\|\Omega_k\| \leq m_{\Omega_k}$ and $\|\Omega_k\| \leq 2m_{\Omega_k}$ then we have:

$$\Pr\left[\gamma_k \tilde{E}_{k1} \phi_k(\hat{e}_k)\right] = \gamma_k \tilde{E}_{k1} \phi_k(\hat{e}_k) - \gamma_k \frac{\tilde{E}_{k1} \Omega_k^T \phi_k(\hat{e}_k)}{\|\Omega_k\|^2} \Omega_k$$

in which $\phi_k(\hat{e}_k) = L_k^{-1}(s)[\varphi_k(\hat{e}_k)]$ with $L_k(s)$ is chosen so that $L_k^{-1}(s)$ the transfer function is stable and even.

To eliminate chattering in the system, the control component u_{nh} is given by [13-16]:

$$u_{nh} = \begin{cases} \rho_k & \text{if } \tilde{E}_{k1} \geq 0 \text{ and } |\tilde{E}_{k1}| > \xi_k \\ -\rho_k & \text{if } \tilde{E}_{k1} < 0 \text{ and } |\tilde{E}_{k1}| > \xi_k \\ \rho_k \tilde{E}_{k1} / \xi_k & \text{if } |\tilde{E}_{k1}| < \xi_k \end{cases} \quad (49)$$

here ξ_k is a positive constant.

5 Simulation Results

The parameters are indicated in Tab. 1:

Tab. 1 Set of hypothetical flight instrument parameters.

TT	Parameter names and symbols	Value	Unit
1	Volume of AFD, m	520	kg
2	Stable flight speed, V_0	280	m/s
3	Programmed flight altitude, H	10	m
4	Cruise engine thrust corresponding to stable flight speed, P	5 600	N
5	Characteristic area, S	0.65	m ²
6	Characteristic length, L	3.85	m
7	Moment of inertia, j_z	380	kg·m ²
8	AFD body diameter, D	0.42	m
9	Mean aerodynamic arc of wing lift, L_c	0.42	m
10	Distance from AFD center of gravity to rudder pressure center, L_{cl}	1.02	m

5.1 Simulation of the System with a PID Controller

From the geometric dynamic model (30) and the assumed parameters in the table above, construct the Simulink diagram for the angular pitch stabilization control system for the AFD with a PID controller as shown in Fig. 4. Use the optimization tool in Simulink to determine K_P , K_I and K_D .

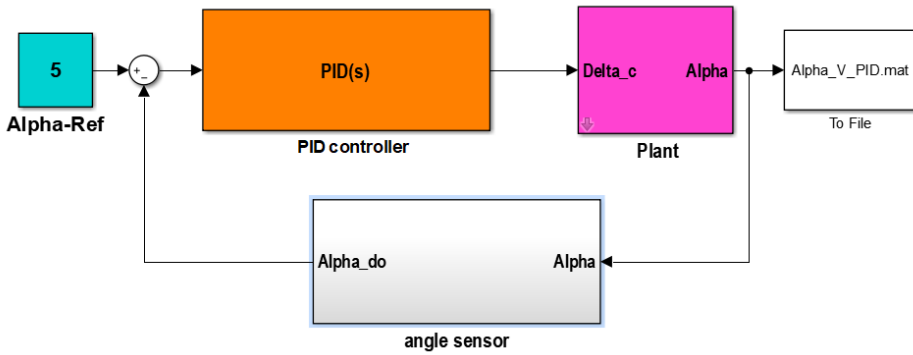


Fig. 4 Simulink diagram for angular pitch stabilization of the AFD using the PID method

5.2 Simulation of the Control System with an LQ Controller

Choose $Q = \begin{bmatrix} 1 & 0 & 0 \\ 0 & 1 & 0 \\ 0 & 0 & 1 \end{bmatrix}$, $R = 1$, with the assumed parameters in Tab. 1. By applying the $lqr(A, B, Q, R)$ function in Matlab, we obtain the parameters of the optimal LQ controller:

$$K_{clq}^T = [-18.34 \quad -4.31 \quad -24.49]$$

Fig. 5 constructs the Simulink diagram according to model (36) and control law (42).

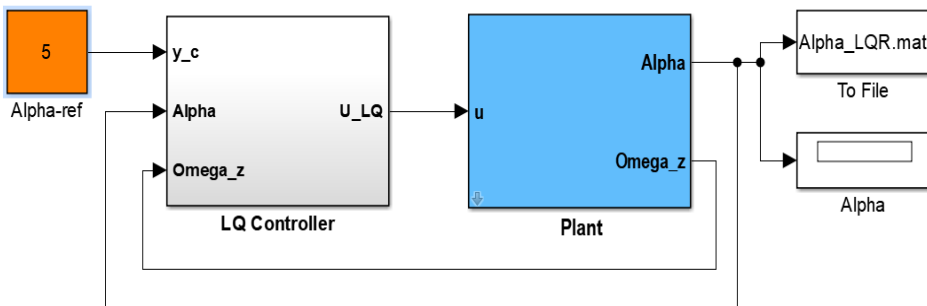


Fig. 5 Angular pitch stabilization system of the AFD using an LQ controller

5.3 Simulation of the Direct Adaptive Controller (NFC)

Based on the dynamic model (30) and the intelligent control algorithm (46), combined with the assumed parameters in Tab. 1, the Simulink diagram simulating the angle of attack stability control algorithm for AFD is constructed as shown in Fig. 6

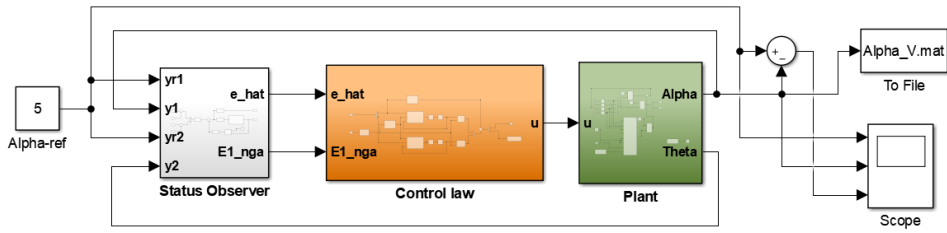


Fig. 6 Simulink diagram simulating the control algorithm

Figs 7-9 show the simulation results of the system errors for the PID controller, LQ controller, and Direct Adaptive Controller (NFC) with a sinusoidal reference signal. Figs 10 and 11 depict the system response and the control response of the system with an initial pitch angle Alpha of 5 degrees. Fig. 12 illustrates the system response when the speed of the AFD increases to 580 m/s at time $t = 20$ s. The sinusoidal signal is chosen to test the system's ability to track the input signal under oscillating signals, while the Alpha of 5 degrees is selected to assess the stability of the system under initial conditions with a specific angle deviation.

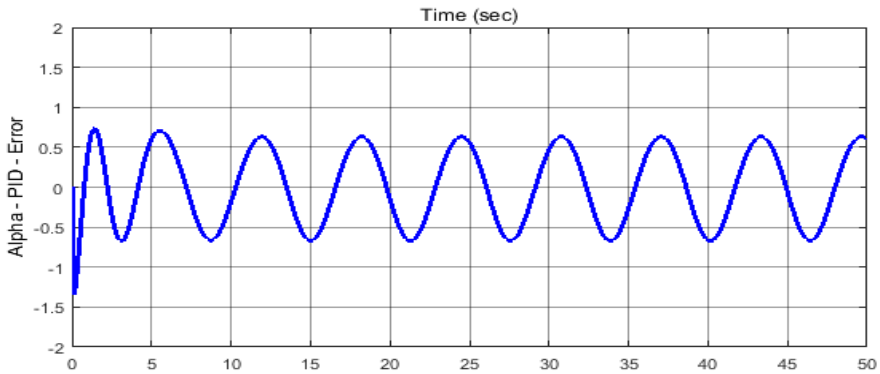


Fig. 7 Response error of the system for the PID controller

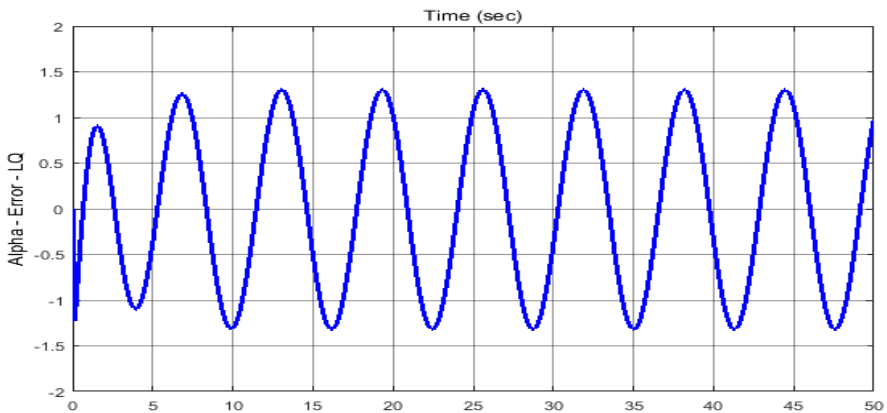


Fig. 8 Response error of the system signal for the LQ controller

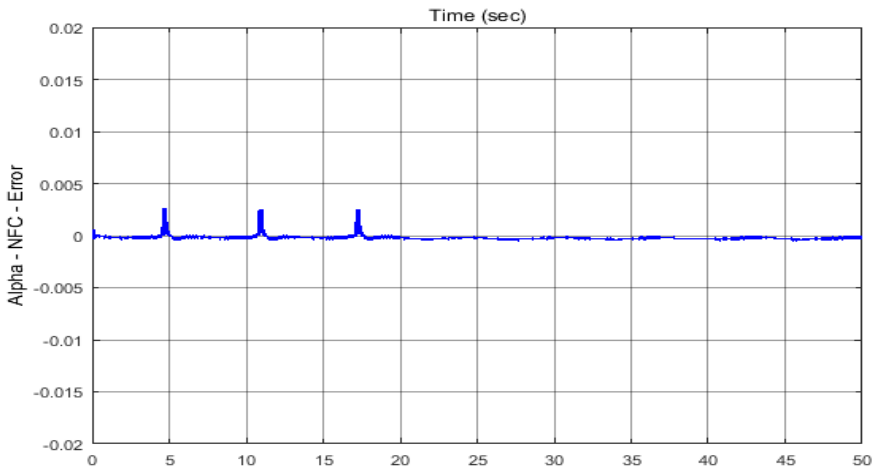


Fig. 9 Response error of the system for the Direct Adaptive Controller (NFC)

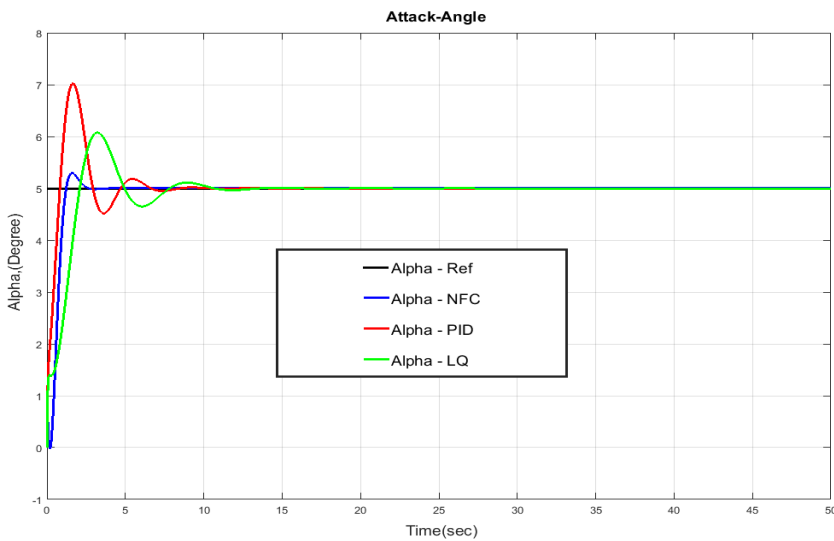


Fig. 10 System response when the reference signal Alpha is 5 degrees

Figs 10 and 11 show the system response, error signal, and control response of the system at the time $t = 20$ s when external disturbance impacts the system (wind impact).

The results presented in Figs 7-9 illustrate the effectiveness of the Direct Adaptive Controller (NFC) when tracking a sinusoidal reference signal. The NFC demonstrated a remarkable ability to minimize the error between the reference signal α and the actual α of the AFD, achieving a high level of accuracy. In contrast, the output responses of both the PID and LQ controllers exhibited significant errors and failed to follow the reference signal α adequately.

These findings highlight that high-precision tracking of the angular pitch (Alpha angle) of the AFD can be achieved using the direct adaptive control algorithm.

Integrating a Neuro-Fuzzy network allows for the estimation of the ideal controller, leveraging online learning capabilities. As observed in Fig. 10, the NFC controller outperforms the PID controller in terms of overshoot, with values of 3 % and 15 %, respectively. Furthermore, the settling time for the NFC controller was shorter than that of both the PID and LQ controllers, indicating superior performance in achieving stability.

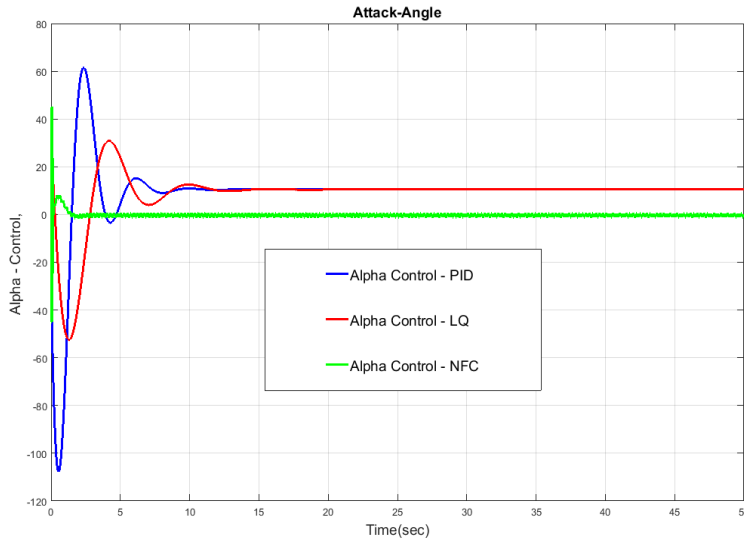


Fig. 11 Control response of the system when the reference signal Alpha is 5 degrees

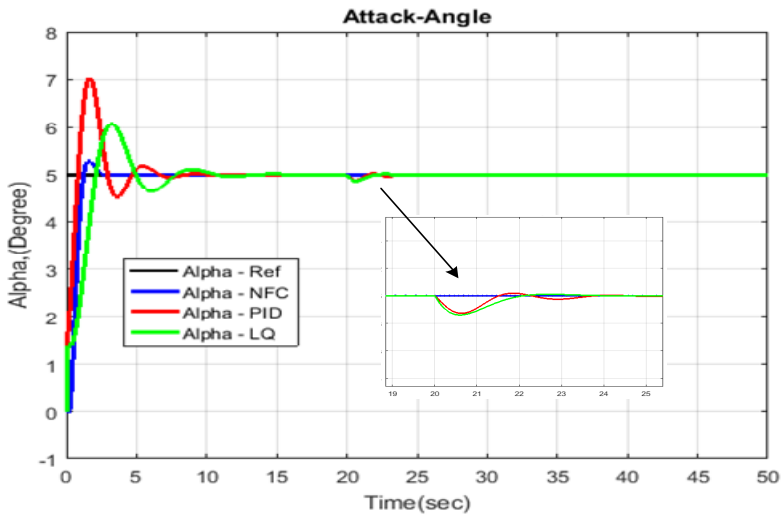


Fig. 12 System response when the speed of the AFD increases to 580 m/s at time $t = 20$ s

In the final motion phases, an experiment was conducted to assess the AFD's response while varying its speed from 280 m/s to 580 m/s. Fig. 12 illustrates that the output responses from the PID and LQ controllers did not adequately track the desired

input. Conversely, the NFC controller maintained accurate tracking of the desired input, showcasing its effective online adaptation capabilities during variations in flight speed.

These results demonstrate the advantages of employing a direct adaptive control strategy, particularly in dynamic environments where the system parameters may change rapidly. Future work will focus on further refining the control algorithms and exploring their applicability in real-time systems.

6 Conclusion

In scenarios where the input signal is sinusoidal or when the Alpha angle is fixed at 5 degrees, the Direct Adaptive Controller (NFC) demonstrates enhanced control performance compared to both the PID and LQ controllers. The simulation results further substantiate that the NFC controller maintains accurate tracking of the input signal during variations in flight speed. This study successfully implements the direct adaptive control algorithm to precisely regulate the pitch angle of the AFD by the desired specifications. The outcomes of the simulations conducted in the Matlab/Simulink environment validate the applicability of the NFC controller for effective tracking of the required pitch angle within a nonlinear model characterized by changing flight speeds.

Despite the favorable simulation results achieved with the direct adaptive control algorithm, further evaluations must be conducted in real-time operational settings. Successful real-time implementation could pave the way for a myriad of applications in AFDs experiencing variable speeds. Additionally, this opens new avenues for research in intelligent control theory aimed at enhancing the precision of control methodologies for a class of aerial vehicles subject to speed fluctuations.

References

- [1] PLAISTED, C.E. *Design of an Adaptive Autopilot for an Expendable Launch Vehicle* [online]. [Master Thesis]. Orlando: University of Central Florida, 2008 [viewed 2024-03-21]. Available from: <https://core.ac.uk/download/pdf/236295986.pdf>
- [2] FAWZY, M., M.A.S. ABOELELA, O. ABD EL RHMAN and H.T. DORRAH. Design of Missile Control System Using Model Predictive Control. *The Online Journal on Computer Science and Information Technology*, 2011, **1**(3), pp. 64-70.
- [3] TURKOGLU, K., U OZDEMIR, M. NIKBAY and E.M. JAFAROV. PID Parameter Optimization of an UAV Longitudinal Flight Control System, *International Journal of Mechanical, Aerospace, Industrial and Mechatronics Engineering*, 2008, **2**(9), pp. 35-40. DOI 10.5281/zenodo.1079352.
- [4] TONG, S., T. WANG and J.T. TANG. Fuzzy Adaptive Output Tracking Control of Nonlinear System. *Fuzzy Sets and Systems*, 2000, **111**(2), pp. 1169-1182. DOI 10.1016/S0165-0114(98)00058-X.
- [5] WANG, L.-X. *Adaptive Fuzzy Systems and Control, Design and Stability Analysis*. Hoboken: PTR Prentice Hall, 1994. ISBN 0-13-099631-9.
- [6] ROVITHAKIS, C.A. and M.A. CHRISTODOULOU. Adaptive Control of Unknown Plans Using Dynamical Neural Network. *IEEE Transactions on Systems, Man, and Cybernetics*, 1995, **24**(3), pp. 400-412. DOI 10.1109/21.278990.

-
- [7] GE, S.S., C.C. HANG, T.H. LEE and T. ZHANG. *Stable Adaptive Neural Network Control*. New York: Springer, 2001. ISBN 1-4419-4932-1.
- [8] ZHANG, T., S.S. GE and C.C. HANG. Adaptive Output Feedback Control for General Nonlinear Systems Using Multilayer Neural Networks. In: *Proceedings of the 1998 American Control Conference*. Philadelphia: IEEE, 1998. DOI 10.1109/ACC.1998.694722.
- [9] HORIKAWA, S., T. FURUHASHI and Y. UCHIKAWA. On Fuzzy Modeling Using Fuzzy Neural Networks with the Back-Propagation Algorithm. *IEEE Transactions on Neural Networks*, 1992, **3**(5), pp. 801-806. DOI 10.1109/72.159069.
- [10] WANG, W.-Y., Y.G. LEU and C.C. HSU. Robust Adaptive Fuzzy-Neural Control of Nonlinear Dynamical Systems Using Generalized Projection Update Law and Variable Structure Controller. *IEEE Transactions on Systems, Man, and Cybernetics, Part B (Cybernetics)*, 2001, **31**(1), pp. 140-147. DOI 10.1109/3477.907573.
- [11] PHAM, Q.H. and T.D. TRAN. Synthesizing an Adaptive Control Law for a Class of Autonomous Aerial Vehicles in the Navy. In: *Proceedings of the International Conference on Advanced Mechanical Engineering, Automation, and Sustainable Development 2021 (AMAS2021)*. Cham: Springer, 2021, pp. 765-769. DOI 10.1007/978-3-030-99666-6_110.
- [12] SIOURIS, G.M. *Missile Guidance and Control Systems*. New York: Springer, 2004. ISBN 0-387-00726-1.
- [13] LABIOD, S., M.S. BOUCHERIT and T.M. GUERRA. Adaptive Fuzzy Control of a Class of MIMO Nonlinear Systems. *Fuzzy Set and Systems*, 2005, **151**(1), pp. 59-77. DOI 10.1016/j.fss.2004.10.009.
- [14] IOANNOU, P.A. and J. SUN. *Robust Adaptive Control* [online]. Hoboken: Prentice-Hall, 1996 [viewed 2024-03-24]. Available from: https://viterbi-web.usc.edu/~ioannou/RobustAdaptiveBook95pdf/Robust_Adaptive_Control.pdf
- [15] WANG, W.-Y., Y.-G. LEU and T.-T. LEE. Output – Feedback Control of Nonlinear Systems Using Direct Adaptive Fuzzy – Neural Controller. *Fuzzy Set and Systems*, 2002, **140**(2), pp. 341-358. DOI 10.1016/S0165-0114(02)00519-5.
- [16] LANDAU, I.D., R. LOZANO, M. MSAAD and A. KARIMI. *Adaptive Control- Algorithms, Analysis and Applications*. London: Springer, 2011. ISBN 0-85729-663-9.